Caltech

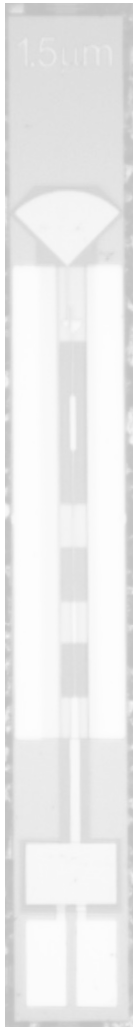

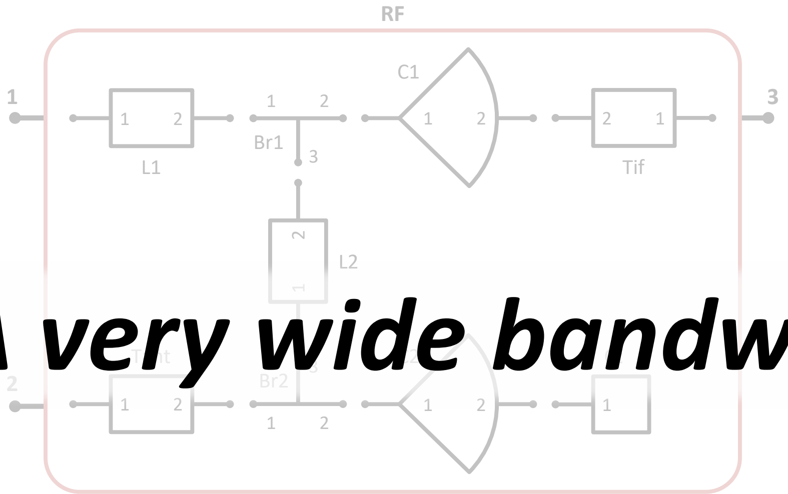

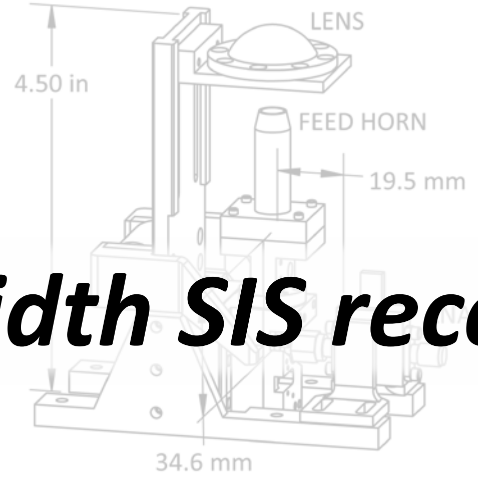

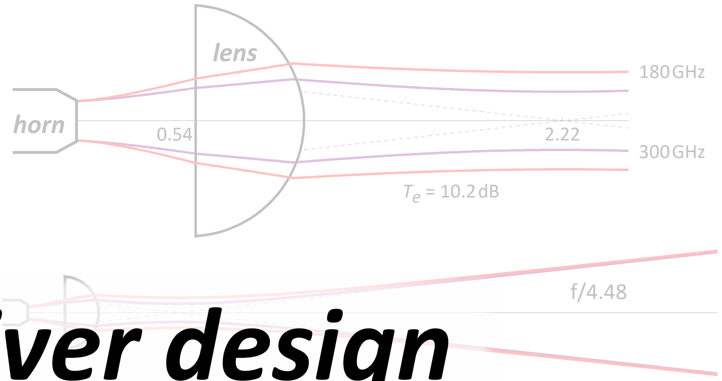

A very wide bandwidth SIS receiver design

Frank Rice

thesis defense August 2020

$$Y_{(m,m')} = \frac{-j}{2(m'V_{ph}+V_{if})}\sum_{k=-\infty}^{\infty} C_{(k)}\,C^{*}_{(k+m-m')}\begin{bmatrix} \mathrm{I}(V_0+kV_{ph}) - \\ \mathrm{I}(V_0+kV_{ph}-m'V_{ph}-V_{if}) + \\ \mathrm{I}^{*}(V_0+(k+m-m')V_{ph}) - \\ \mathrm{I}^{*}(V_0+(k+m-m')V_{ph}+m'V_{ph}+V_{if}) \end{bmatrix}.$$

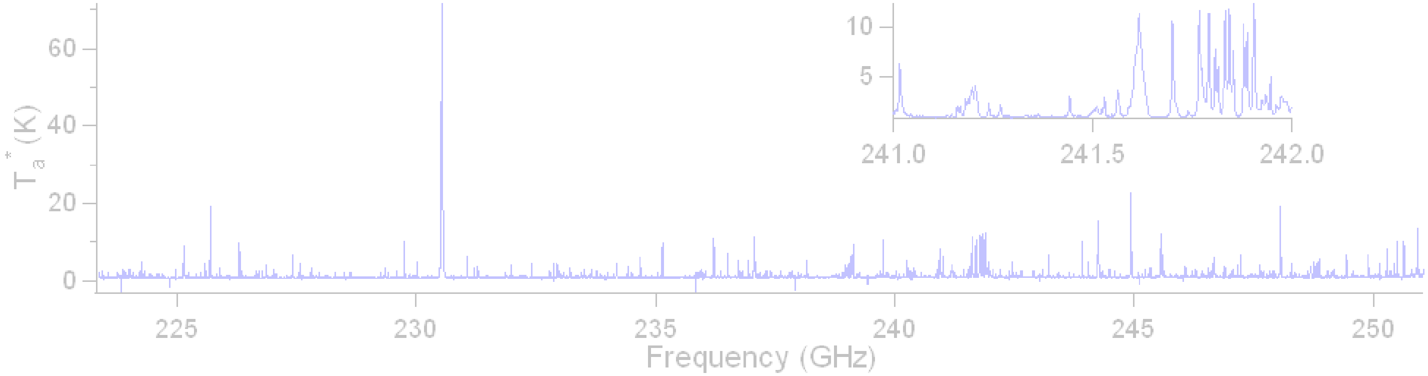

Heterodyne system components

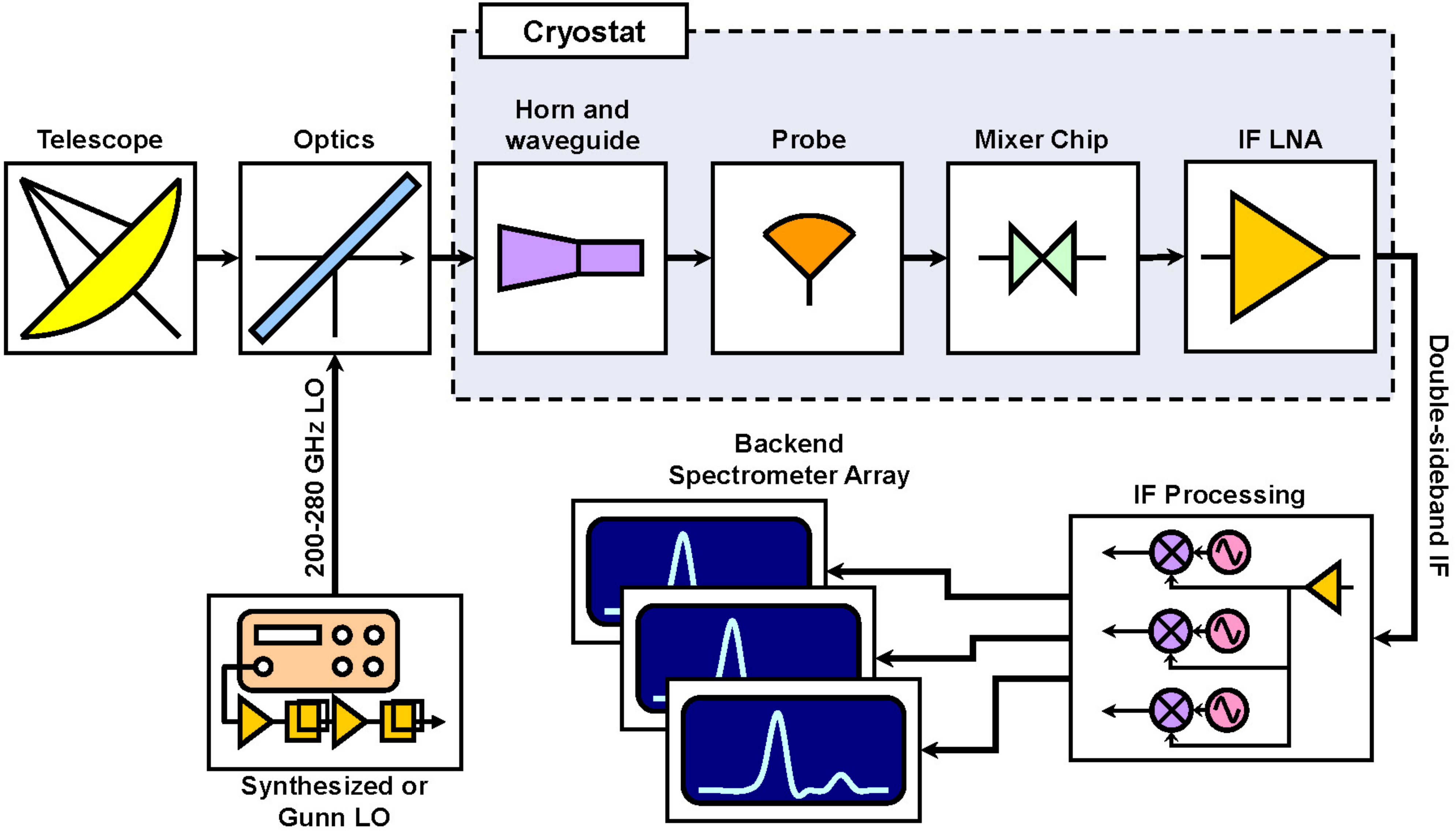

Heterodyne, phase-coherent receiver characteristics

Heterodyne receiver: an astronomical receiver which uses *heterodyne* detection. In addition to the receiver's requirement for a high-power, stable, low-noise, and tunable local oscillator (LO) source, the *phase coherence* between its RF signal input and its IF output has three important consequences: first, the receiver can be designed to have very high frequency resolution, making it ideal for spectrometry; second, the receiver is unfortunately limited in sensitivity by *quantum noise*; third, a single IF output from the receiver can respond to only one component of polarization in the incoming radiation from a source, so that half the power from an unpolarized astronomical source will be undetectable.

Quantum noise: quantum noise provides a limit to the sensitivity of any phase-coherent amplifier such as a heterodyne receiver. It may be roughly thought of as arising due to "spontaneous emission" at the output of a high-gain, coherent amplifier, the desired response being the "stimulated emission" of the amplifier output in response to the signal input. In the case of a heterodyne detector, it is the input RF frequency (not the much lower IF frequency) which determines the system's *quantum noise limit*. The quantum noise limit corresponds to an equivalent *noise temperature* of 10 K at 208 GHz and is proportional to frequency.

A brief, biased history of mm and submm heterodyne SIS receivers

(emphasizing Tom Phillips's and Caltech's roles)

SIS heterodyne receiver history

1970: Wilson, Jefferts, and Penzias detect **CO (1-0) at 115 GHz** using a Schottky diode mixer, using the NRAO 36' telescope with a receiver designed by Sandy Weinreb. Detections from Orion as well as several other sources.

1971: At Penzias's suggestion, T. Phillips begins work on a InSb hot-electron bolometer-based heterodyne receiver. Receiver covers 100-600 GHz, but only has a 1 MHz IF bandwidth. He and Jefferts make first detection of **CO (2-1)** at 230 GHz and then **CO (3-2)** at 345 GHz (this latter line using the Palomar 200" telescope).

1975: Still at Bell Labs, **Phillips suggests using an SIS device for a heterodyne detector**.

1979: Phillips comes to Caltech and begins work with Bob Leighton on CSO. Phillips, Dolan, Woody use a Bell Labs, lead alloy, **SIS junction in a 115 GHz heterodyne receiver at OVRO**.

1979: **John Tucker** (Aerospace Corp., later U. Illinois) publishes his quantum mixing theory, with immediate application to SIS devices, which he did in 1980.

1980-1985: Phillips and collaborators use KAO to find many lines 460-626 GHz using InSb receiver on KAO.

1986: **CSO completed**. Phillips becomes its director.

1986: G. Blake, E. Sutton and others complete the **first ever 230 GHz line survey** (of Orion) using an SIS receiver at OVRO (Bell Labs lead alloy junction).

1987: First niobium-based SIS receivers designed by Tony Kerr at NRAO installed on Kitt Peak 12m telescope.

1992: Nb-based 230 GHz SIS receiver installed at CSO.

1998: 850 GHz SIS receiver developed for CSO.

2009: Hershel space telescope with HIFI heterodyne receiver suite: 5 SIS-based bands covering 480-1250 GHz. two HEB-based receivers cover 1410-1910 GHz.

2003: ALMA (Atacama Large MM/SubMM Array) begins construction. SIS-based, 66 antenna interferometer (54 12m diameter, 12 7m diameter).

My receiver development timeline

1997: Joined J.Z.'s group; began work on SuperMix.

1999: SuperMix validated; first version released. Receiver design concept developed. Began work on probe.

2000: Project approved and funded. Admitted to candidacy. SuperMix development continues. Detailed mixer design studies begin. Dec.: hired by Caltech and began grad student sabbatical.

2002: Probe design completed (Kooi et al. paper in 2003). Mixer chip, mixer block designs completed, cryostat delivered, active LO amplifier-multiplier chain delivered.

2003: Mixer chip delivered (JPL). Mixer block delivered. 15 August: first lab operational check of LO/mixer/LNA system. 28 August: first light at CSO.

2004: Upgraded mixer chip, LNA, RF optics. Gunn LO applied. March: 2^{nd} CSO run. First wide-band, extragalactic spectra obtained.

2005: Major receiver mixer and optics upgrades. Observers begin using the receiver for high-resolution line surveys.

2007: Feb.: receiver to Caltech and back to CSO after quick repair. Last trip away from CSO until retirement. Took over design and management of new CSO facility receiver control and bias electronics.

2012: Mixer chip damaged from too many thermal cycles. Receiver retired from use.


Enrico Sacchetti © 2010

Mixer and cold, focal-plane system design

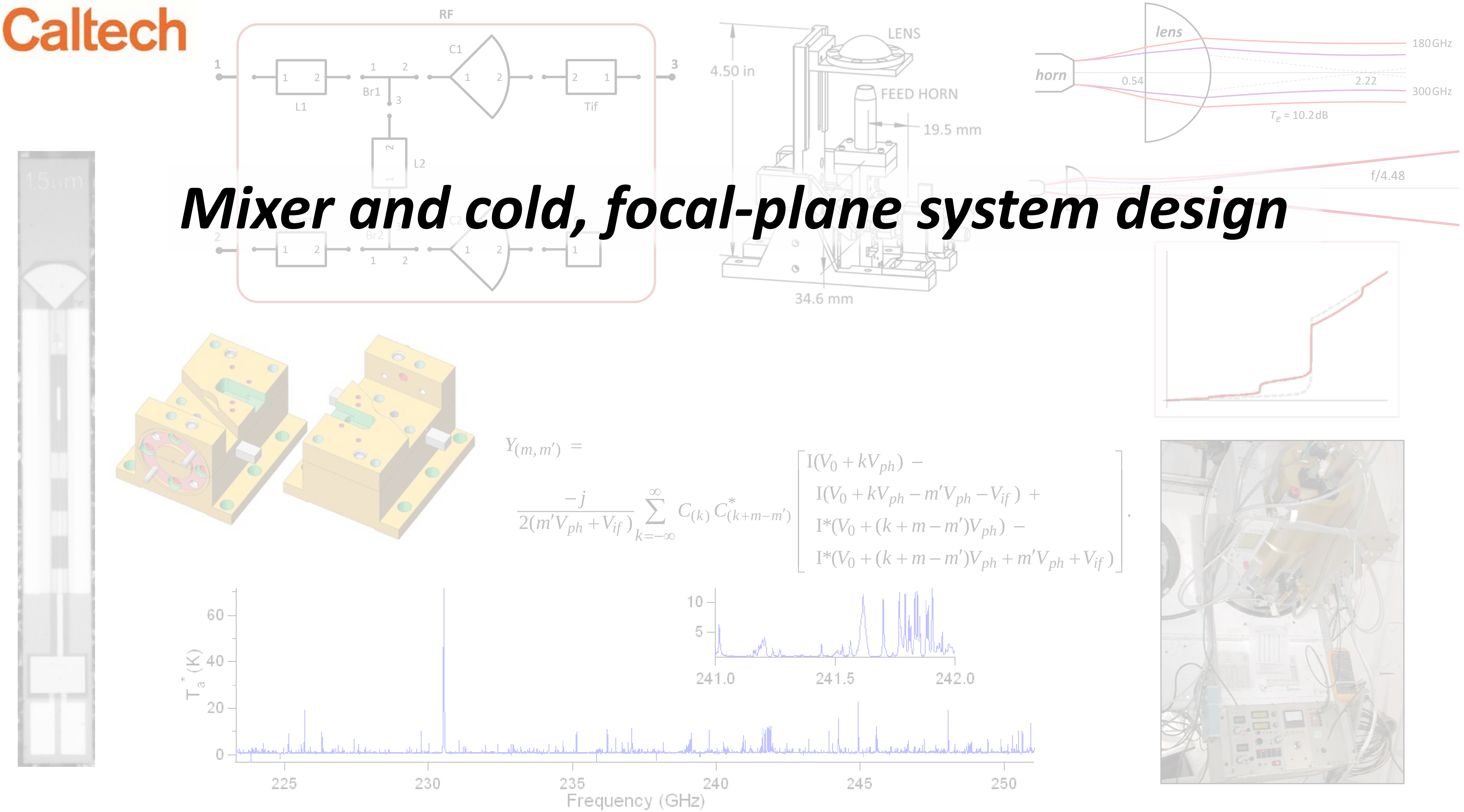

Representing quasiparticle states and transitions

Energies of qp. states near μ

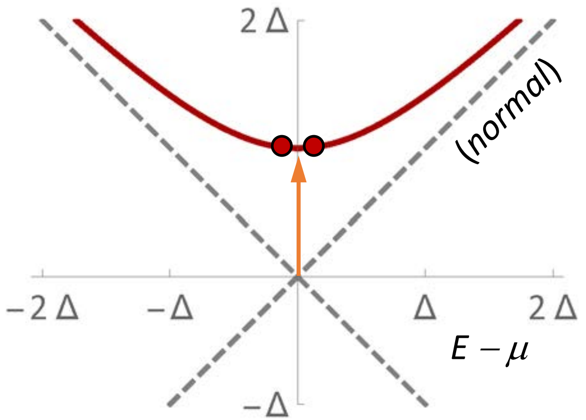

"Semiconductor" representation
density of states near μ

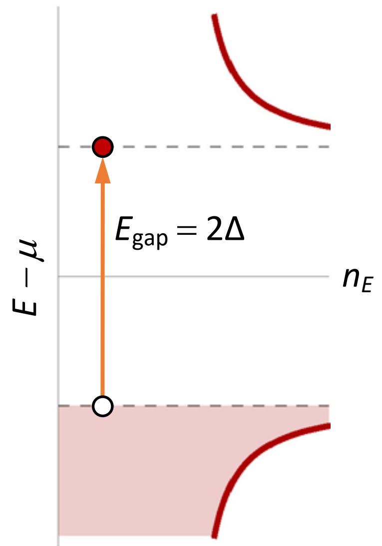

(after I. Giaever [1960])

Niobium characteristics

- Z = 41, W = 93
- $\mu \approx E_F = 5.3$ eV
- E_{gap} = 2Δ = 2.8 meV (Nb) ≈ E_F/2000
- T_C = 9.2K
- Type II, H_C = 0.8T (equiv.)

(cf. Tinkham [1996])

SIS DC I-V characteristic behavior

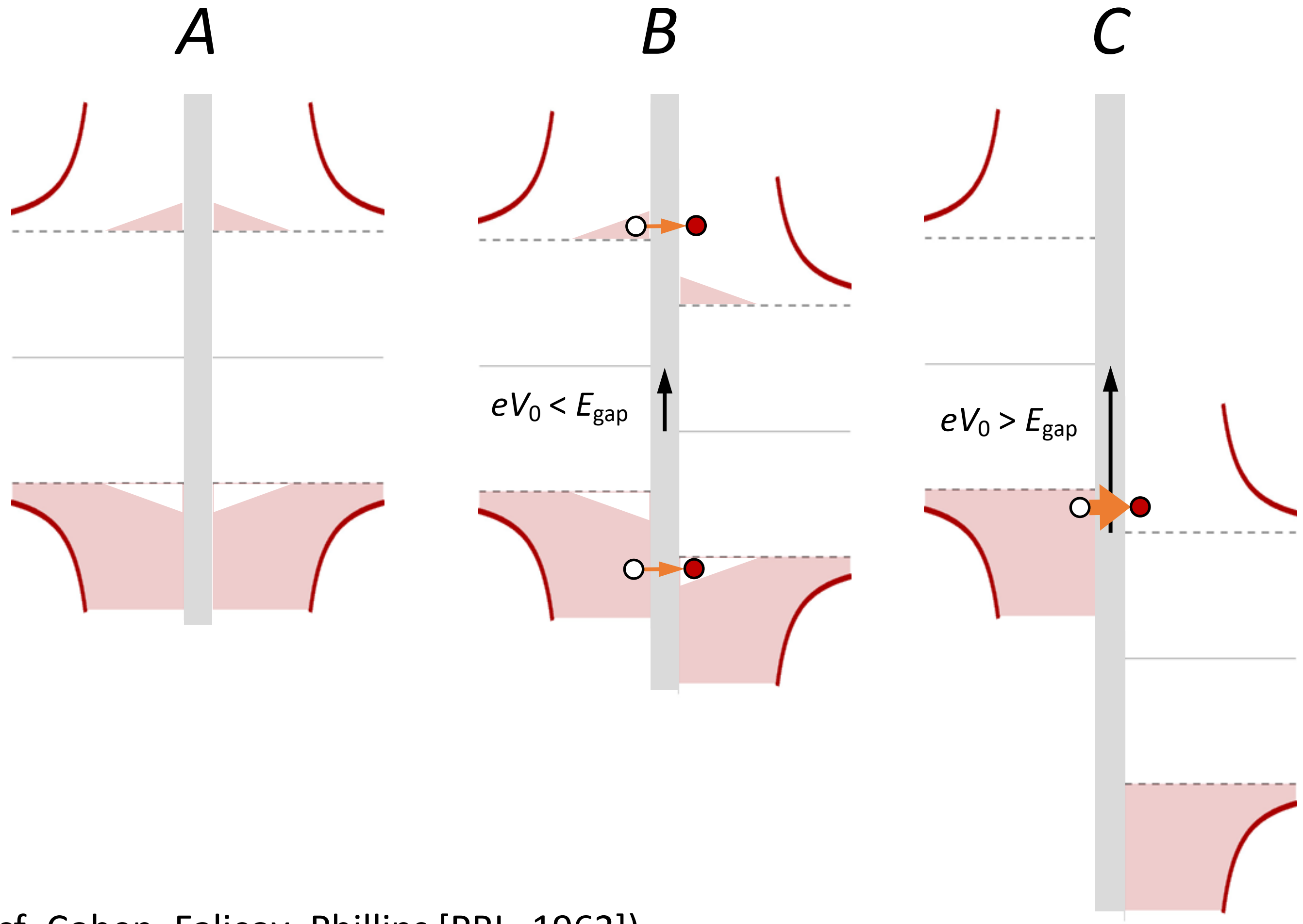

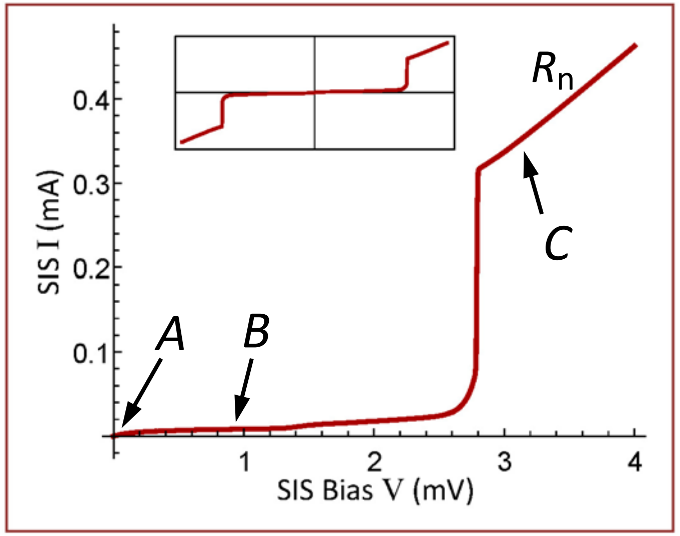

$E_{gap} = eV_{gap} = 2.8\text{meV}$

$R_n = 7.7\text{ohm}$

(cf. Cohen, Falicov, Phillips [PRL, 1962])

LO-pumped SIS DC I-V characteristics

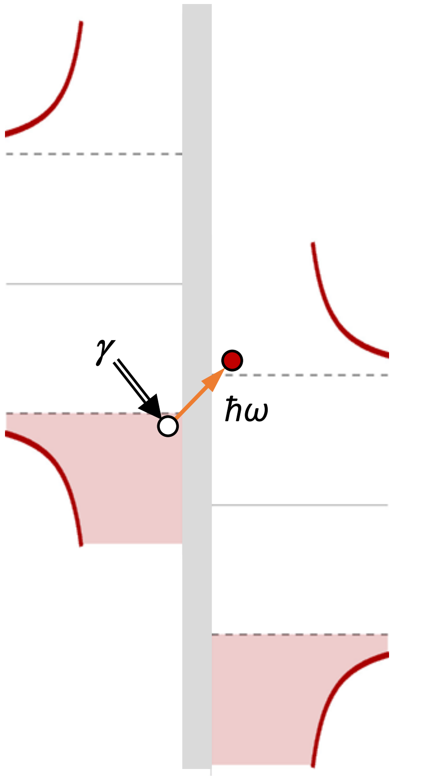

$$i_0(V_0) = J_0(\alpha)^2\, \mathrm{I_{dc}}(V_0) + J_1(\alpha)^2 \left[\mathrm{I_{dc}}(V_0 - V_{ph}) + \mathrm{I_{dc}}(V_0 + V_{ph})\right] + \ldots$$

$$\approx \mathrm{I_{dc}}(V_0) + \tfrac{1}{4}\alpha^2 \left(\left[\mathrm{I_{dc}}(V_0 + V_{ph}) - \mathrm{I_{dc}}(V_0)\right] - \left[\mathrm{I_{dc}}(V_0) - \mathrm{I_{dc}}(V_0 - V_{ph})\right] \right)$$, 2nd difference at V_0

$$\sim \mathrm{I_{dc}}(V_0) + \tfrac{1}{4}\alpha^2 (V_0 + V_{ph})/R_\mathrm{n}$$, V_0 on first photon step (*A*)

$$\sim \mathrm{I_{dc}}(V_0) - \tfrac{1}{4}\alpha^2 V_{ph}/R_\mathrm{n}$$, V_0 within a photon step above V_{gap} (*B*)

(Tucker[1979])

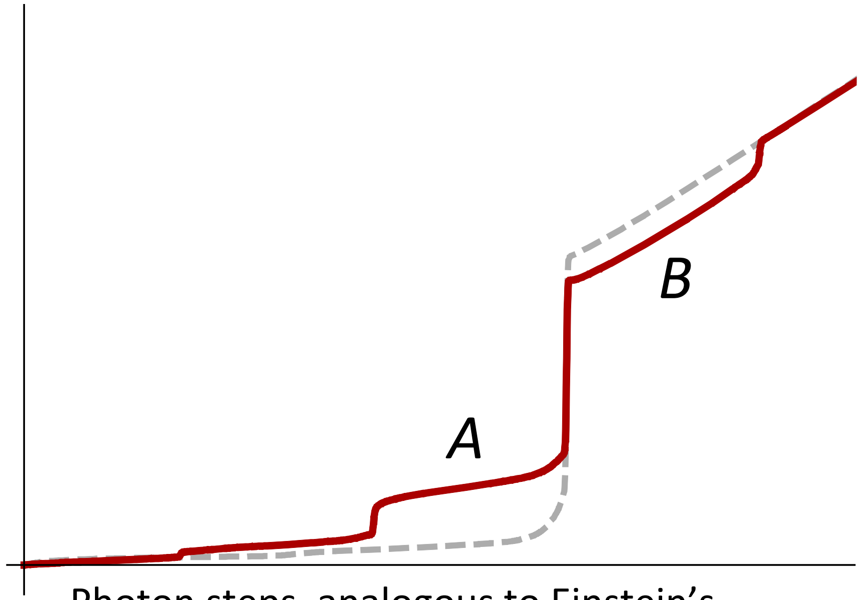

Photon steps, analogous to Einstein's photoelectric effect (Dayem and Martin [1962])

$$J_0(\alpha)^2 \approx 1 - \tfrac{1}{2}\alpha^2 + \ldots$$

$$J_1(\alpha)^2 \approx \tfrac{1}{4}\alpha^2 + \ldots$$

Comparison to observed pumped I-V

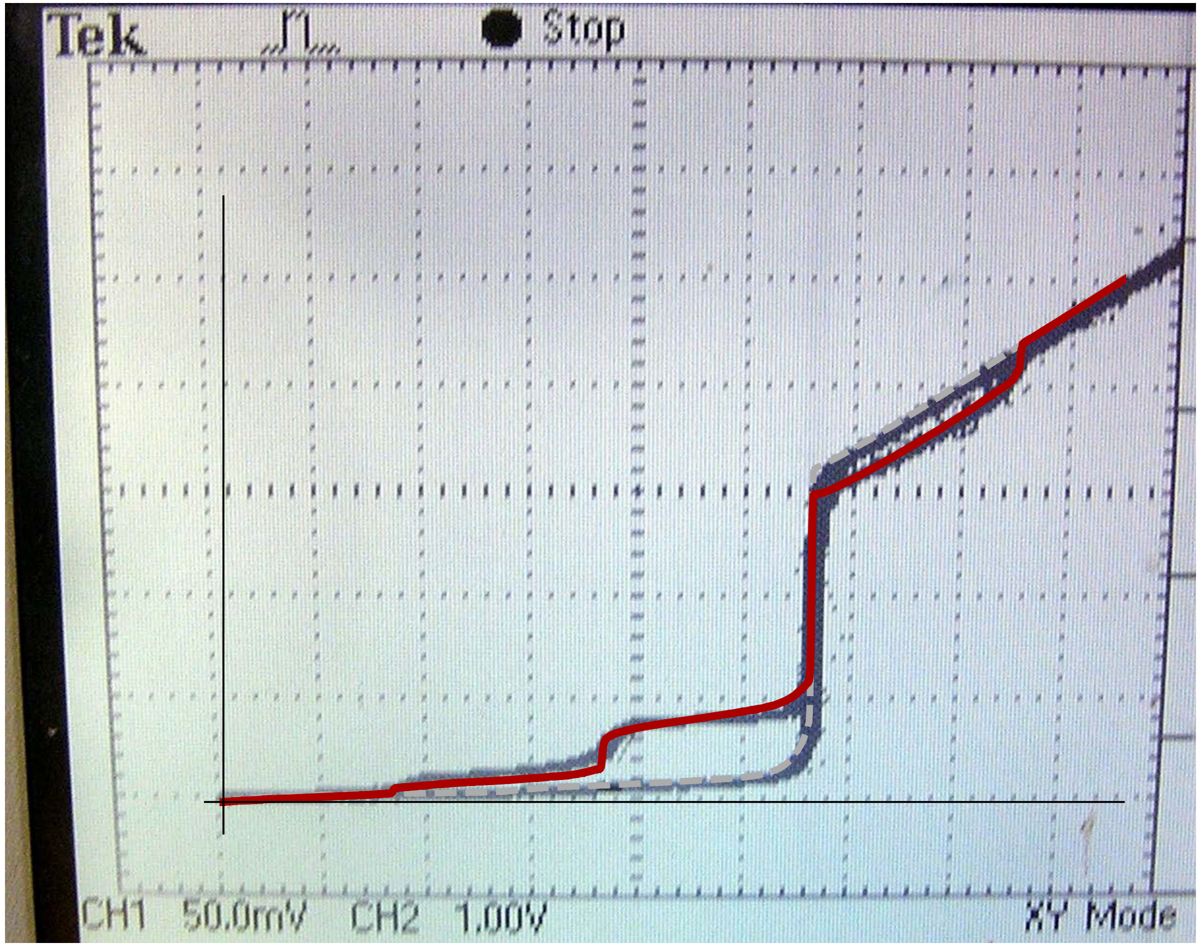

Receiver at CSO, Nov. 2005;
SuperMix model 240 GHz, “α” 0.9

SIS complex admittance at RF frequencies

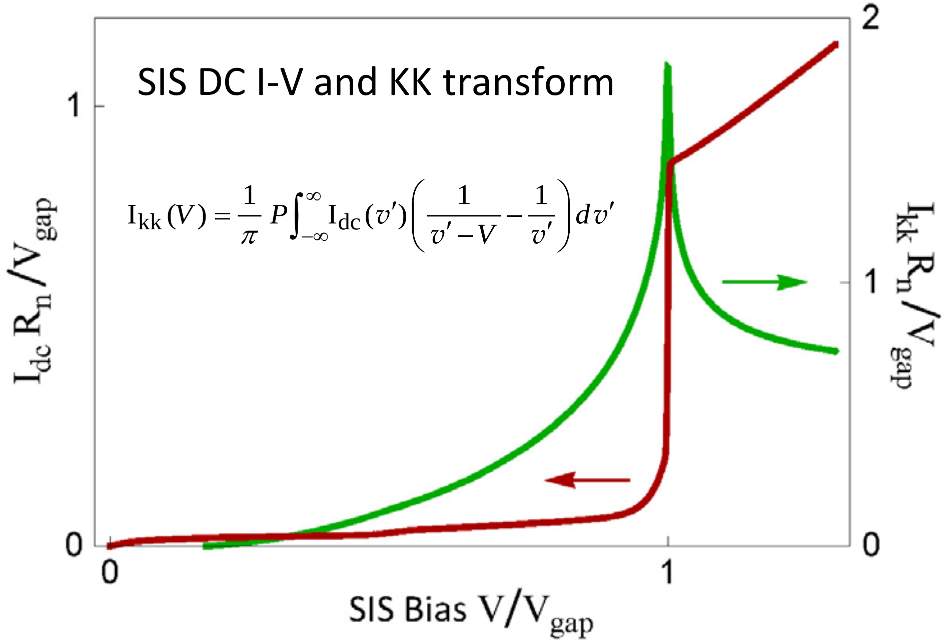

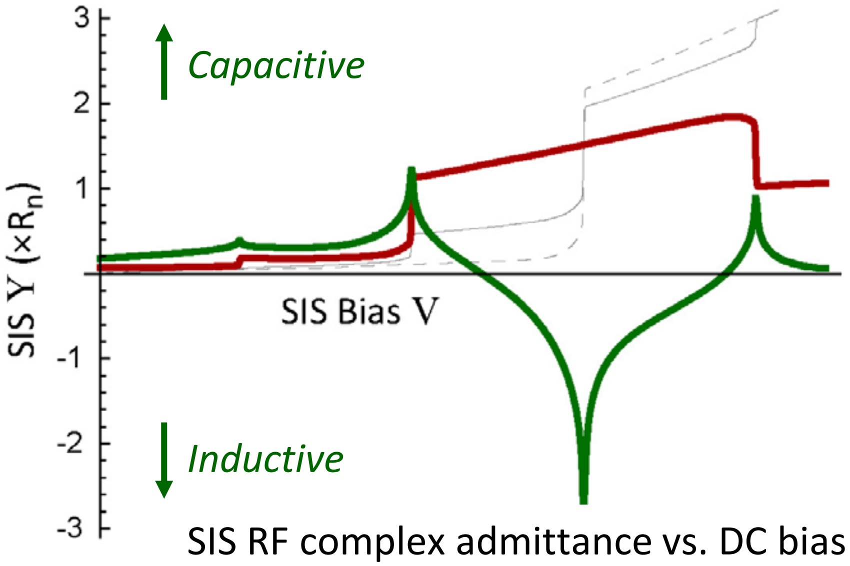

$$i_1(V_{LO}) = J_0(\alpha) J_1(\alpha)\left[I_{dc}(V_0+V_{ph}) - I_{dc}(V_0-V_{ph})\right] + j\, J_0(\alpha) J_1(\alpha)\left[I_{kk}(V_0-V_{ph}) - 2I_{kk}(V_0) + I_{kk}(V_0+V_{ph})\right]$$

(Tucker[1979])

$$\approx 0.3V_{LO} \underbrace{\left[\frac{I_{dc}(V_0+V_{ph}) - I_{dc}(V_0-V_{ph})}{V_{ph}}\right]}_{\text{1st finite difference of } I_{dc} \text{ around } V_0} + j\, 0.3V_{LO} \underbrace{\left[\frac{I_{kk}(V_0-V_{ph}) - 2I_{kk}(V_0) + I_{kk}(V_0+V_{ph})}{V_{ph}}\right]}_{\text{2nd finite difference of } I_{kk} \text{ around } V_0}$$

Reflection, coupling, Smith chart review

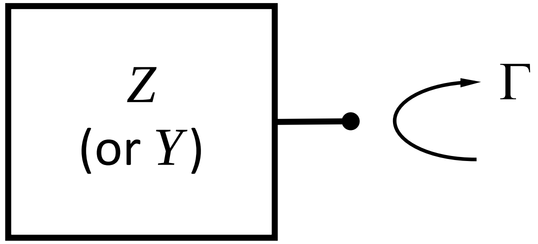

$$\Gamma(\omega) = \frac{Z(\omega) - Z_0}{Z(\omega) + Z_0} = \frac{1 - Z_0\,Y(\omega)}{1 + Z_0\,Y(\omega)}$$

If $\mathrm{Re}(Z \text{ or } Y) < 0$, then $|\Gamma| > 1$
- reflection gain and instability

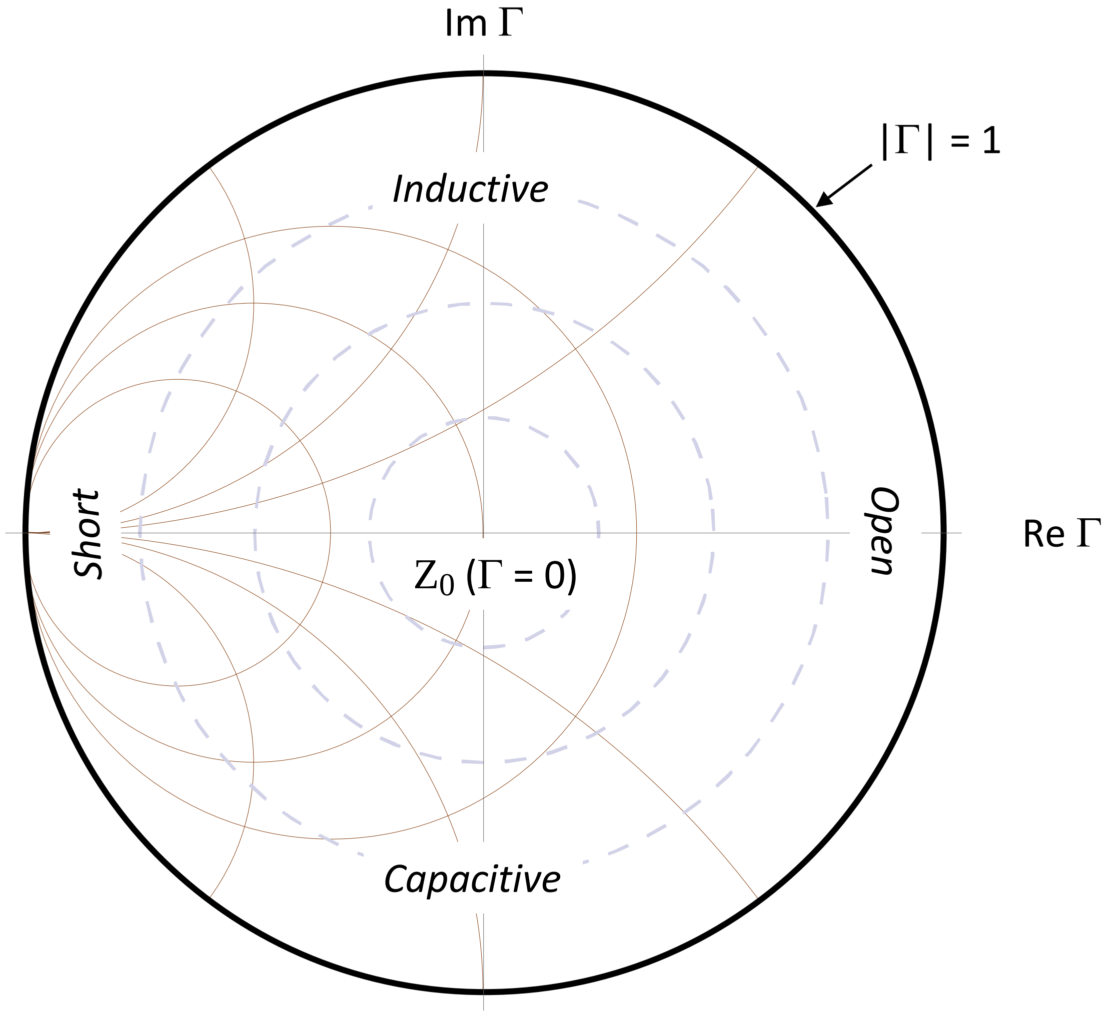

Shown here is a Smith "Y"-type chart: the brown arcs show the map of the admittance half-plane onto the Γ plane

Origin of SIS mixer IF output instability

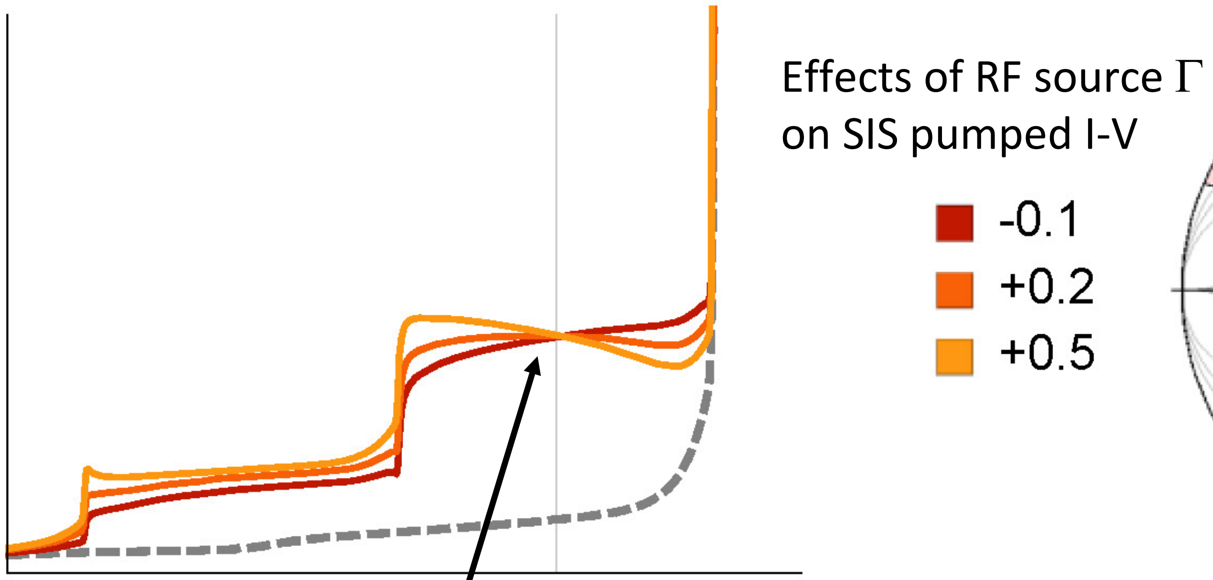

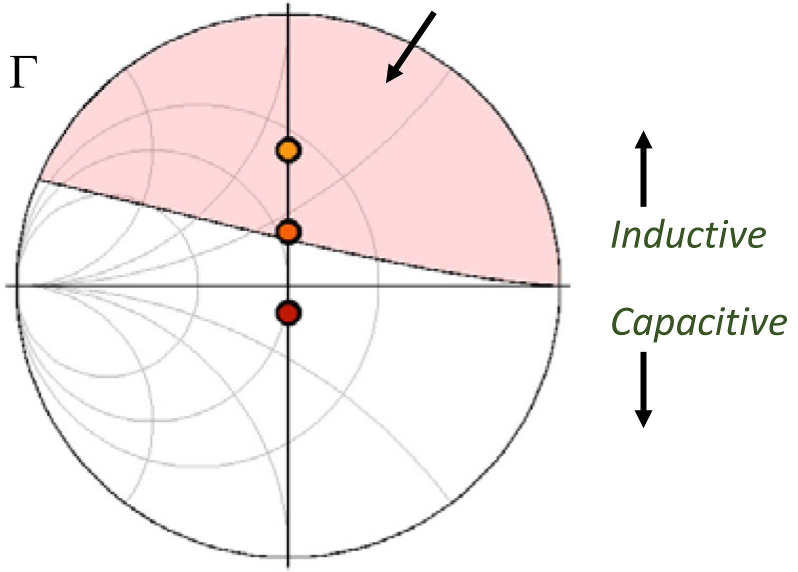

If the RF source has an inductive term, then coupling efficiency degrades as SIS also becomes more inductive (DC bias approaches V_{gap}), giving pumped I-V a negative slope at the selected DC bias voltage.

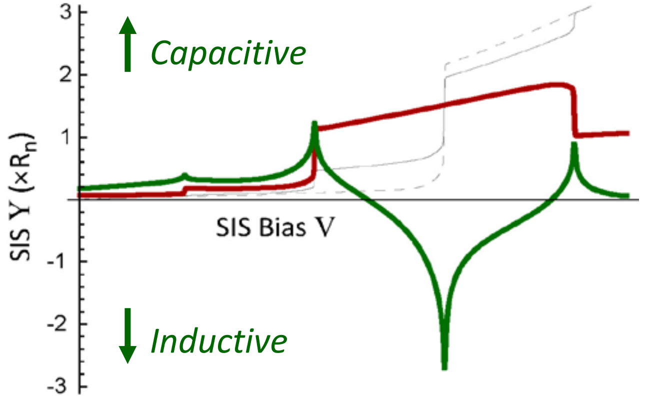

SIS mixer RF-IF conversion efficiency

$$Y_{0,\pm1} = J_0(\alpha) J_1(\alpha) \left[\frac{\mathrm{I_{dc}}(V_0 + V_{ph}) - 2\mathrm{I_{dc}}(V_0) + \mathrm{I_{dc}}(V_0 - V_{ph})}{V_{ph}} \right]$$

$Y_{0,\pm1}$ is maximized (at this level of approximation) if $\alpha = 1.08$ and $J_0(\alpha) J_1(\alpha) = 0.34$.

then: $Y_{\pm(1,1)} \approx (1 - j\, 0.1)/R_{\mathrm{n}}$ and $Y_{0,\pm1} \approx 1.2/R_{\mathrm{n}}$

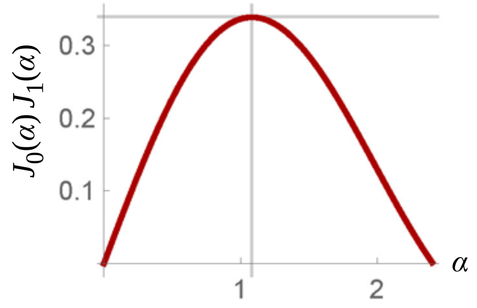

∴The SIS IF current has the same magnitude as the RF signal current.

But the dynamic SIS resistance at the IF frequency, given by the pumped I-V slope at the DC bias point, is ≫ R_{n}, whereas the RF resistance ≈ R_{n}.

Thus SIS IF output power can be greater than the RF input power – an impossible result according to classical theory.

Mixer noise characterization review

Example: simple, DSB mixer model

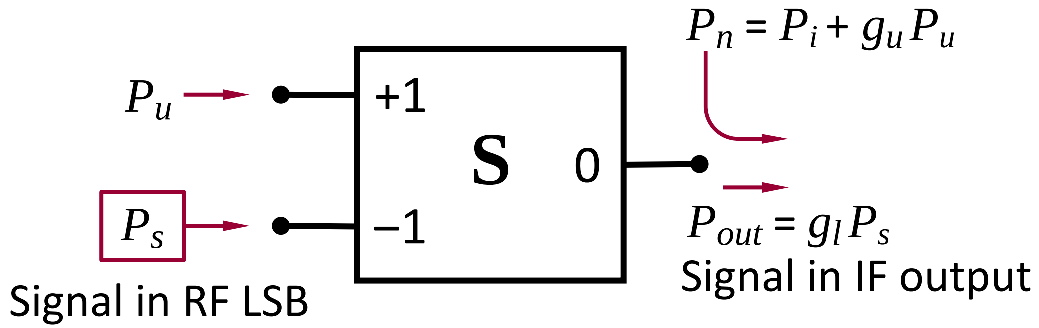

$$T_n(\nu) \equiv \frac{1}{k_B}\frac{dP_n}{d\nu}\bigg|_{\nu(\text{input-referred})}$$

In this case, output noise is divided by LSB power gain, g_l, to get T_n.

"Noise" as analyzed here is considered to result from two random processes:

1. Fluctuations in the flow of current caused by the discrete nature of electric charge (*shot noise*).
2. Fluctuations introduced by the quantum nature of the excitations of the (bosonic) normal mode frequencies of the input channels to the system or from internal dissipative elements (*Bose-Einstein thermal noise* and *quantum noise*).

Phase-coherent amplification and quantum noise

Even at zero temperature, each bosonic wave mode will exhibit ground-state amplitude fluctuations. Phase-coherent amplification responds to the instantaneous amplitude of the source. Such a system's *equivalent input noise power* must therefore be augmented by including this response to bosonic ground-state *quantum "noise"* fluctuations:

$$k_B T_n \equiv \left.\frac{dP_n}{d\nu}\right|_{\substack{\text{input-}\\\text{referred}}} = \left(\frac{h\nu}{\exp(h\nu/k_B T)-1} + \frac{h\nu}{2}\right) = \frac{h\nu}{2}\coth\left(\frac{h\nu}{2k_B T}\right)$$

(Callen and Welton [1951])

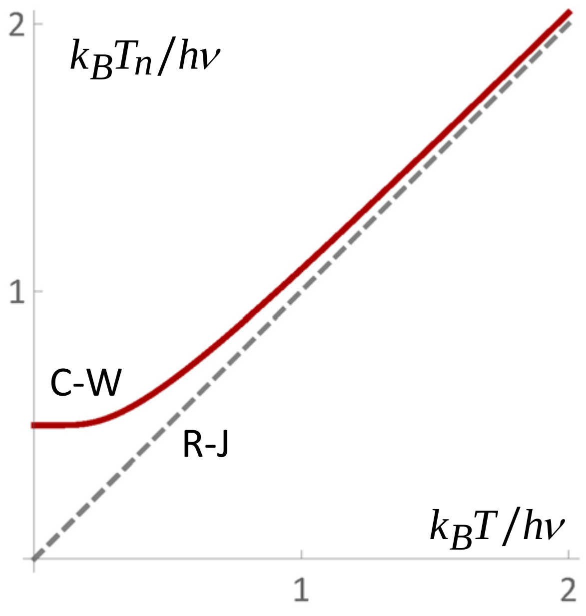

Phase-insensitive, coherent amplifiers add yet another term:

$$T_n(\nu) \geq \underbrace{\frac{h\nu}{2k_B}}_{\substack{\text{C-W}\\\text{noise}}} + \underbrace{\frac{h\nu}{2k_B}\left|1-\frac{1}{G}\right|}_{\substack{\text{minimum possible}\\\text{noise added by amplifer}}} = \underbrace{\frac{h\nu}{k_B}\left|1-\frac{1}{2G}\right|}_{\substack{\text{valid for}\\ G\geq 1}}$$

(Caves [1982])

In DSB mixers, this comes from bosonic fluctuations at the unused sideband inputs. (Wengler [1988])

Optimal RF and IF embedding impedances

RF:

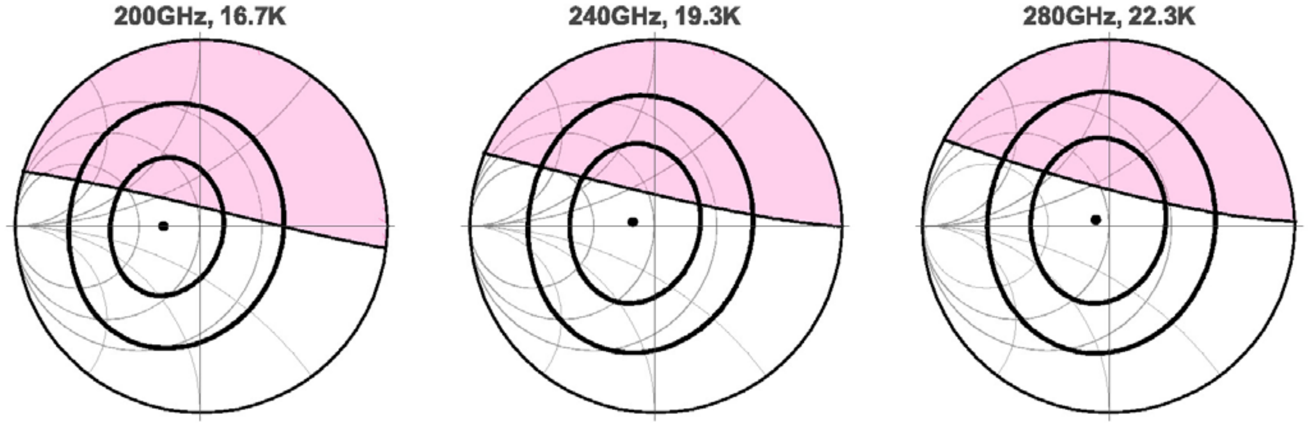

$\alpha = 1.0$; DC bias at the center of the photon step; Smith charts' normalizing impedance is R_n. Mixer T_n contours at 2 and 3 $h\nu_{LO}/k_B$.

IF:

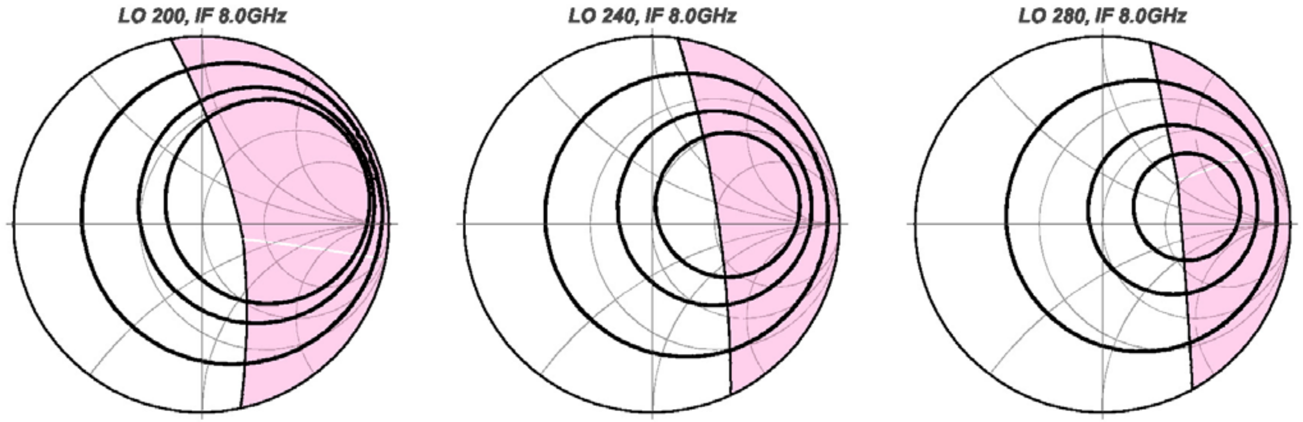

RF embedding Z is $0.8\,R_n$; normalizing impedance is $3R_n$. Mixer RF USB gain contours of −3, 0, and +1 dB.

SIS mixer chip

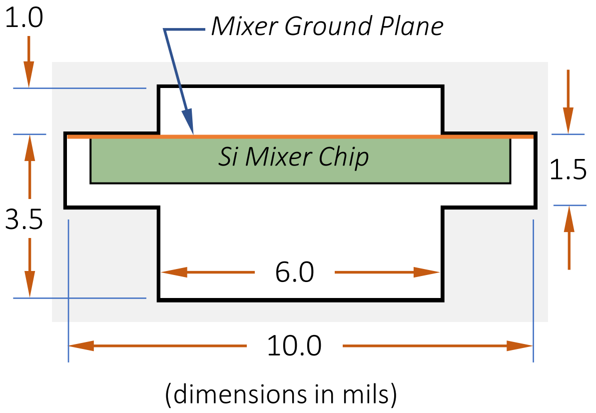

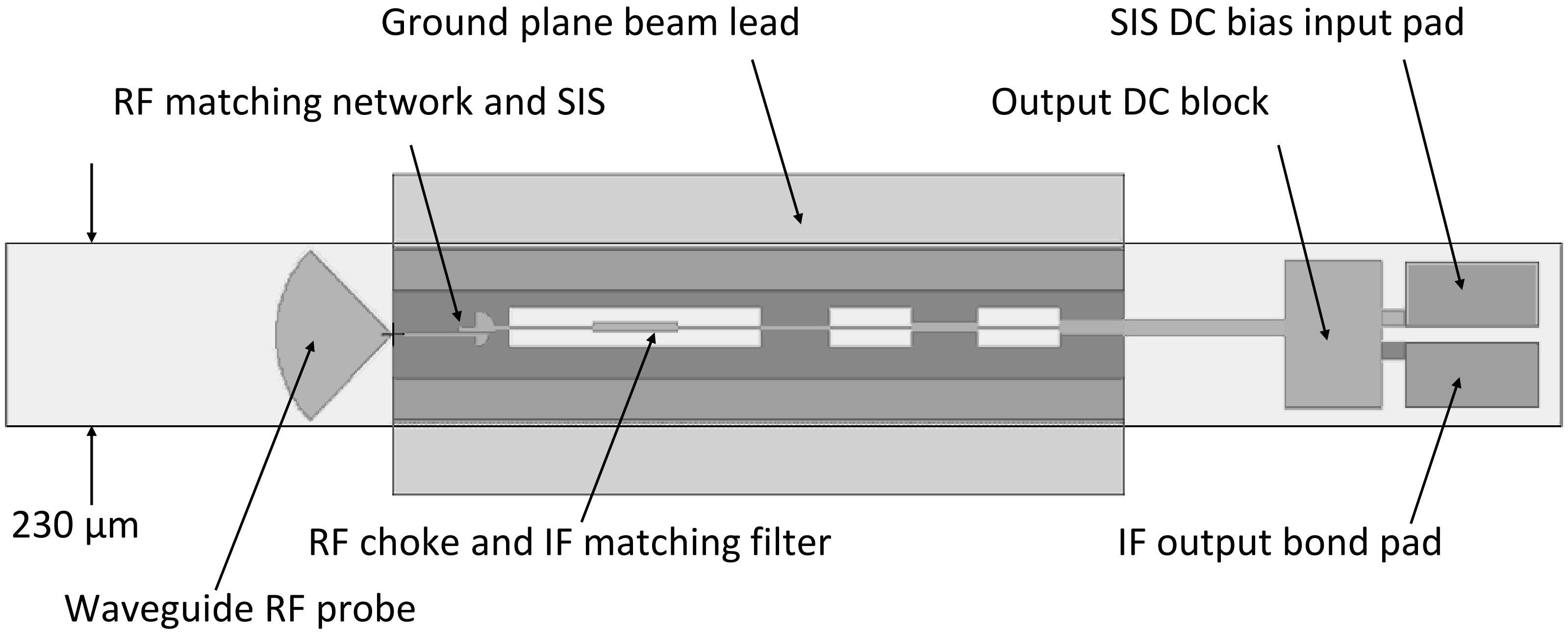

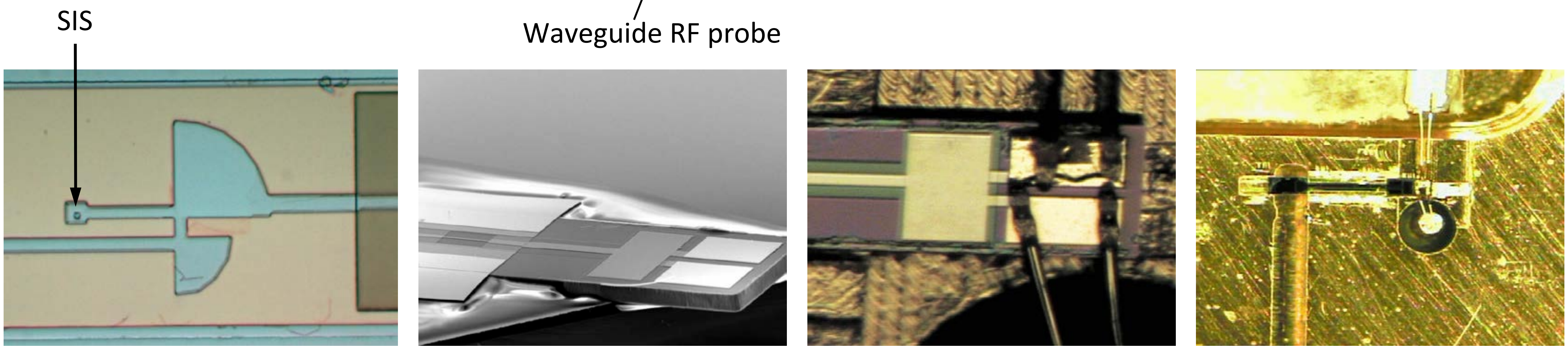

Waveguide probe design

Now the de facto world-wide standard

- Kooi et al. (2003) got the word out early
- *Google Scholar* lists 99 citations, a dozen of which were published in 2017 or later.

(dimensions in mils)

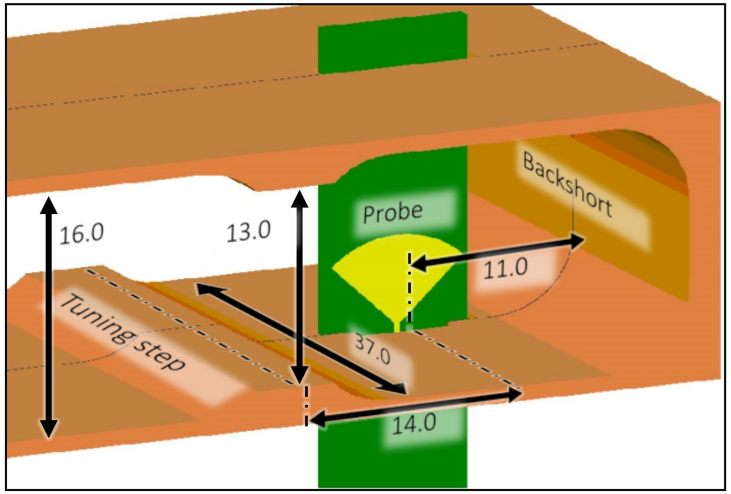

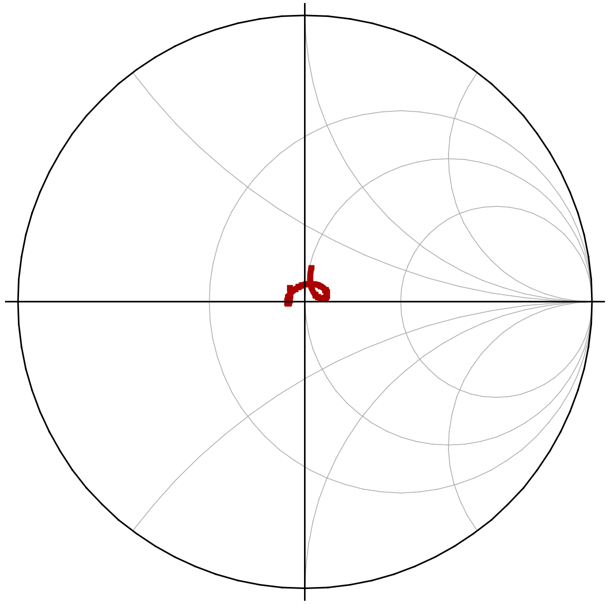

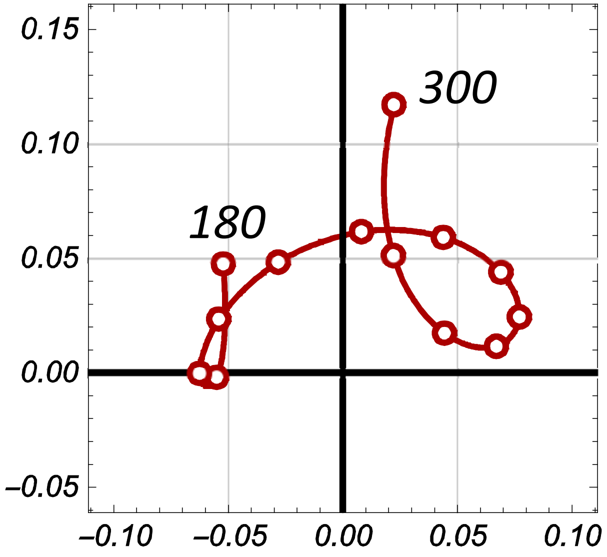

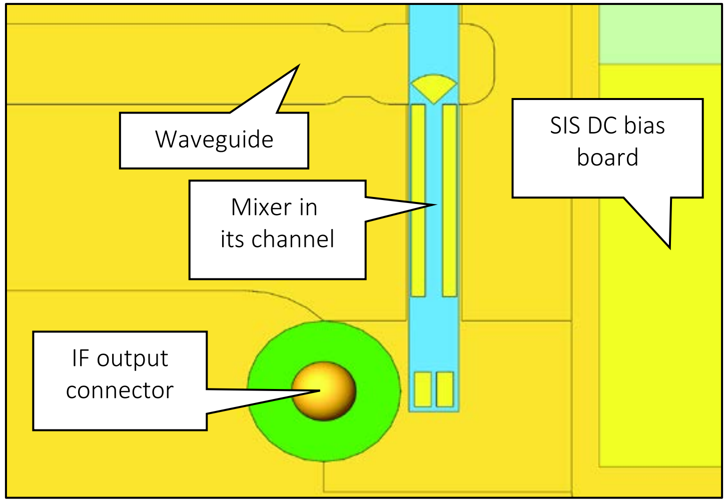

Mixer chip design results (modeled)

(upper) RF embedding impedance normalized to the SIS R_n.

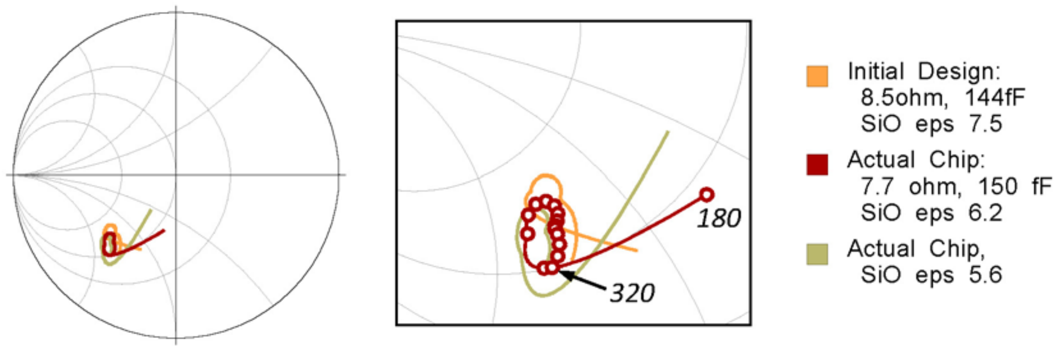

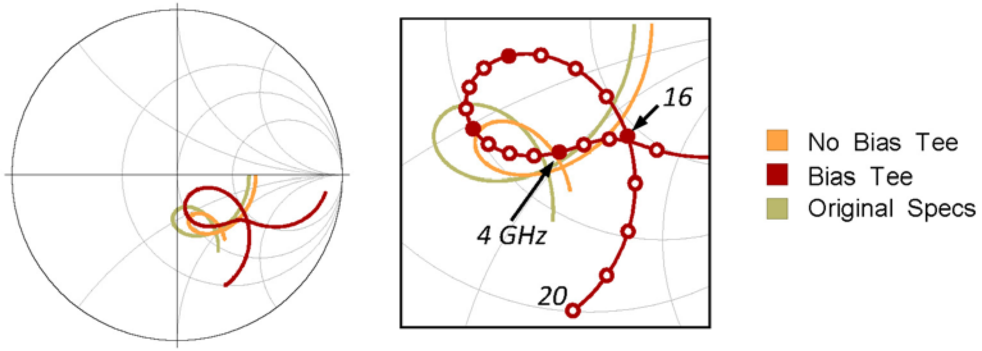

(lower) IF embedding impedance from 0.1 GHz to 20 GHz normalized to 3× R_n.

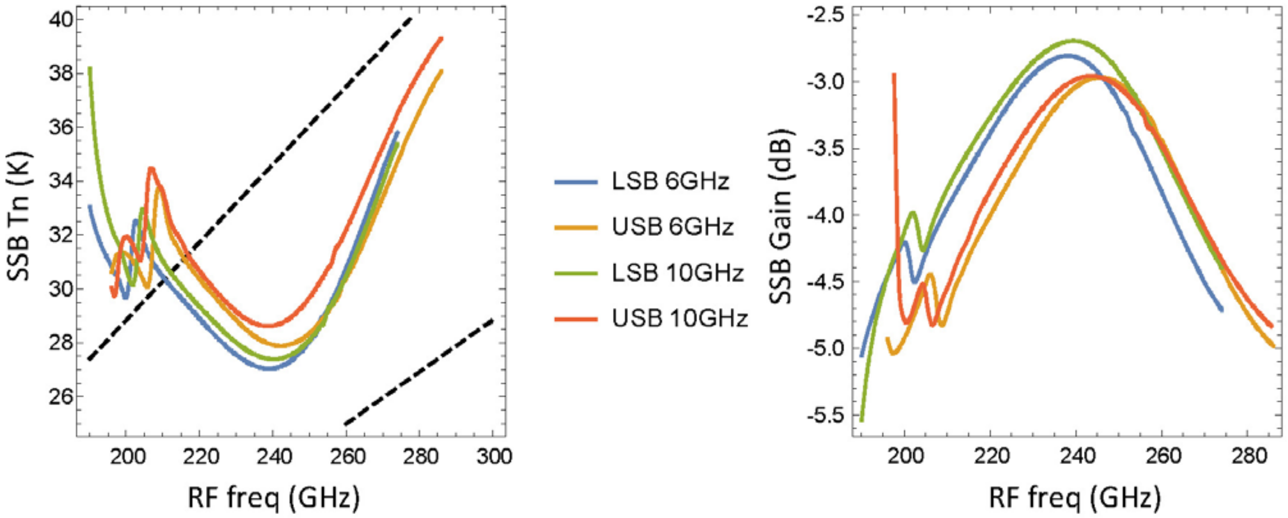

Modeled mixer chip + LNA performance. SiO dielectric constant 5.6. USB and LSB for IF frequencies of 6 and 10 GHz. The RF frequencies are the actual sideband frequencies, $\nu_{LO} \pm \nu_{IF}$. The dashed lines show 2× and 3× the quantum limit noise temperatures (10 K at 208 GHz).

Optimal RF and IF embedding impedances

RF:

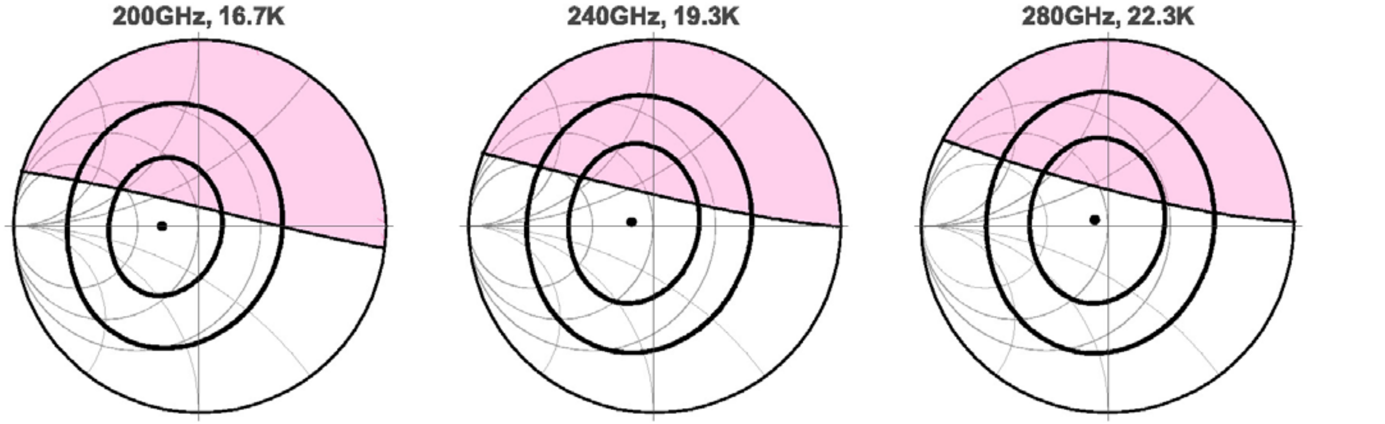

$\alpha = 1.0$; DC bias at the center of the photon step; Smith charts' normalizing impedance is R_n. Mixer T_n contours at 2 and 3 $h\nu_{LO}/k_B$.

IF:

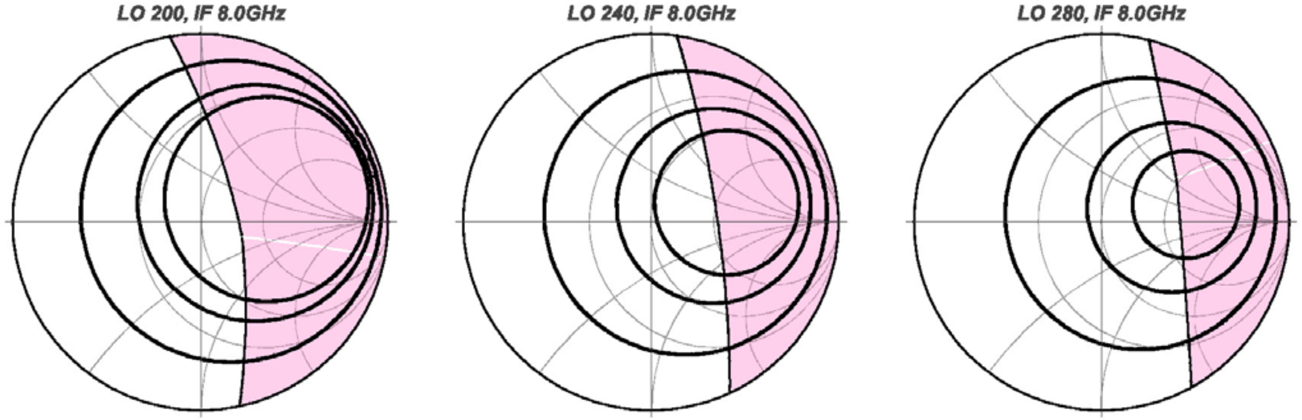

RF embedding Z is $0.8R_n$; normalizing impedance is $3R_n$. Mixer RF USB gain contours of −3, 0, and +1 dB.

Focal plane unit and optics

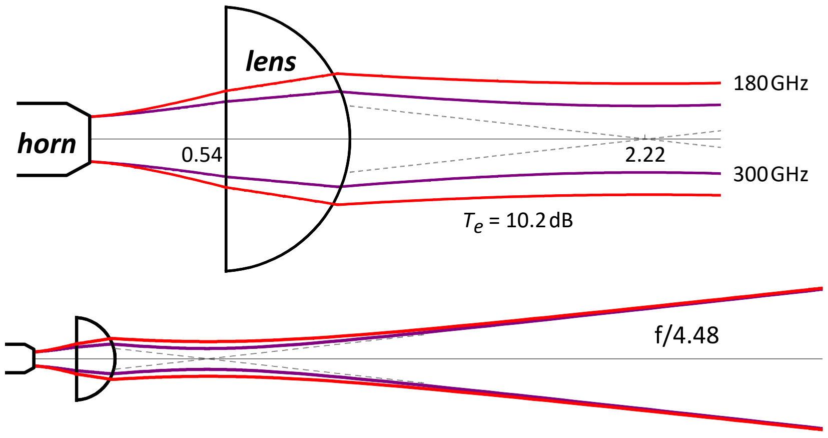

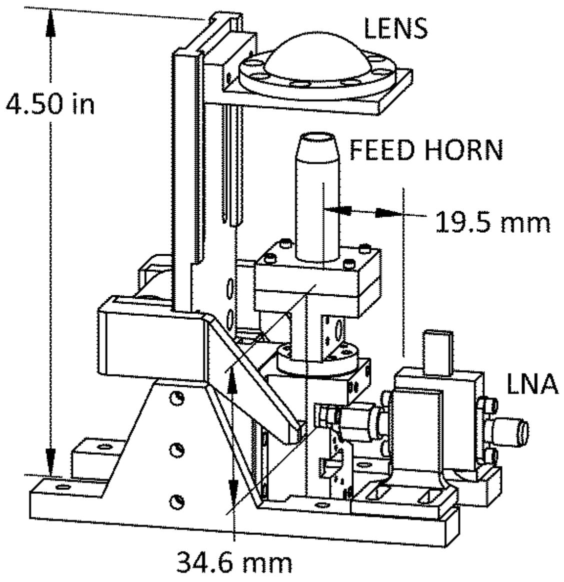

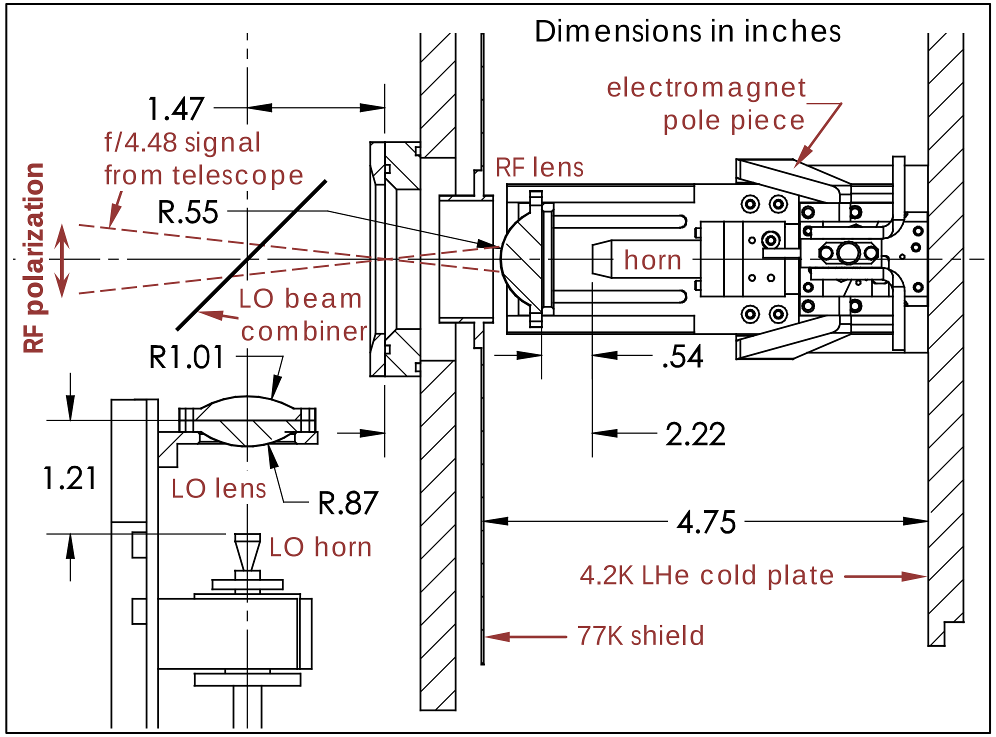

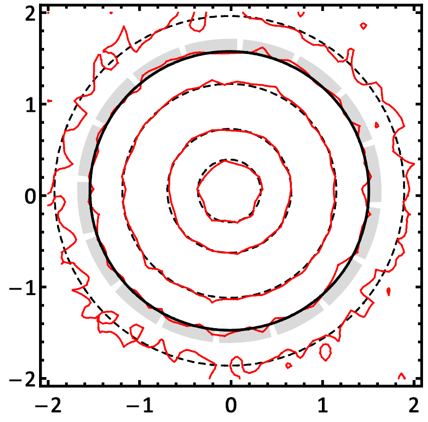

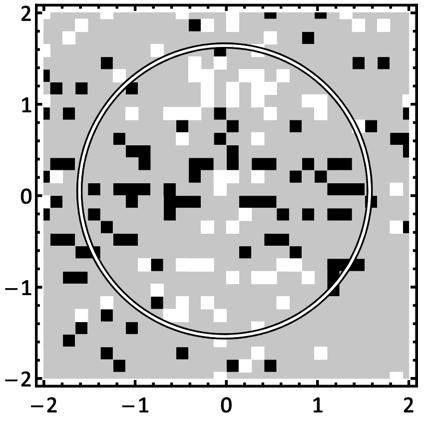

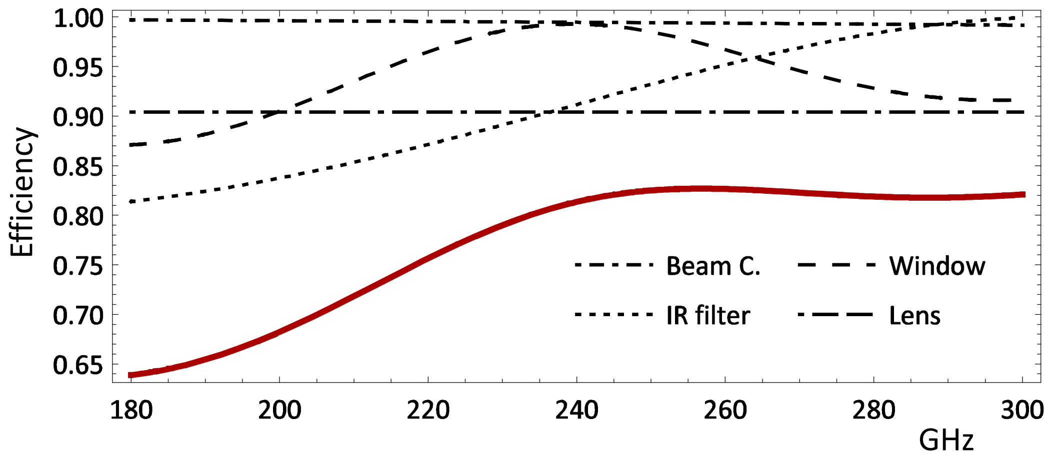

Rx configuration

Lab noise data

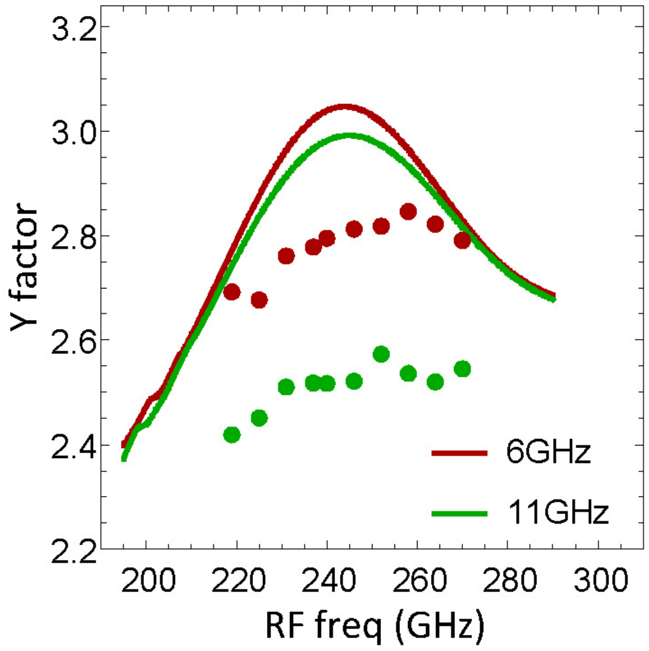

SuperMix-generated Y-factor predictions for complete receiver vs. measured values from 2007. Gunn diode LO and IF output frequency bands of 4–8 GHz and 9.25–13.25 GHz (the latter first down-converted to 4–8 GHz).

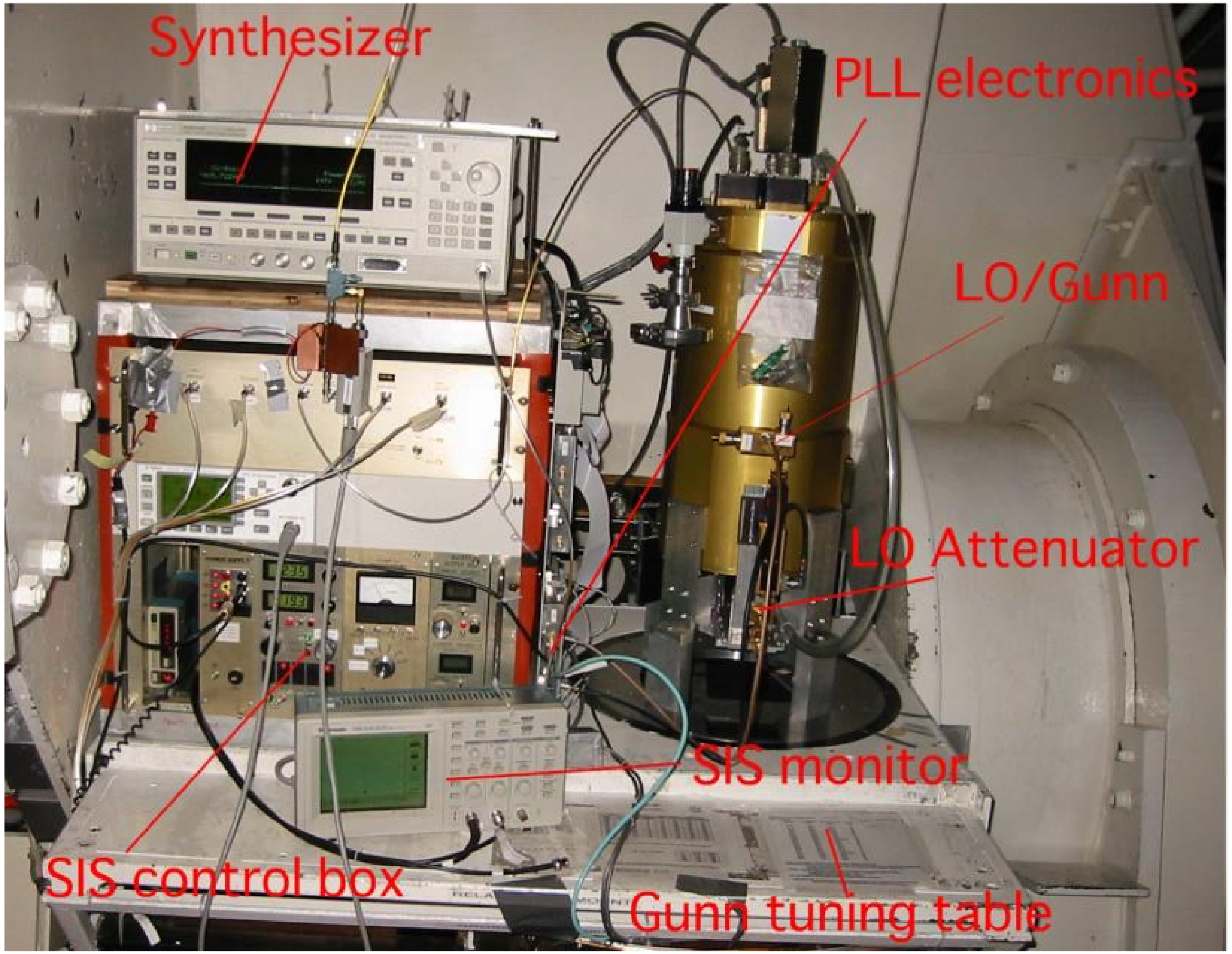

	Facility CSO Rcvrs	Z-Rex
T_{sys} (K, SSB)	120	100
IF Bandwidth (GHz)	1	4

cf. Prof. Susanna L. Widicus Weaver, et al. [2009]

Caltech

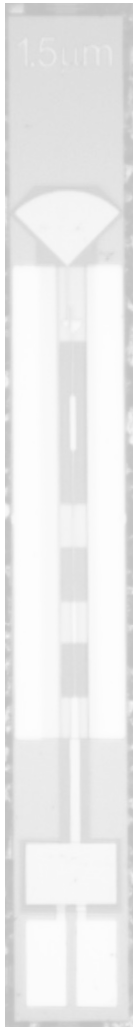

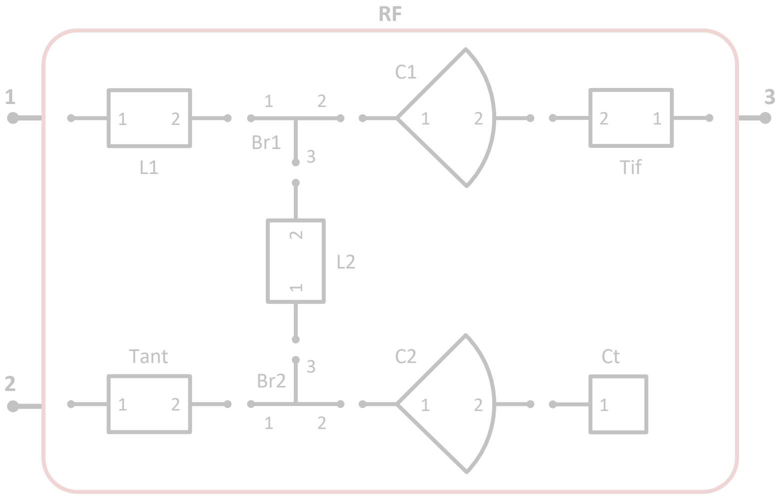

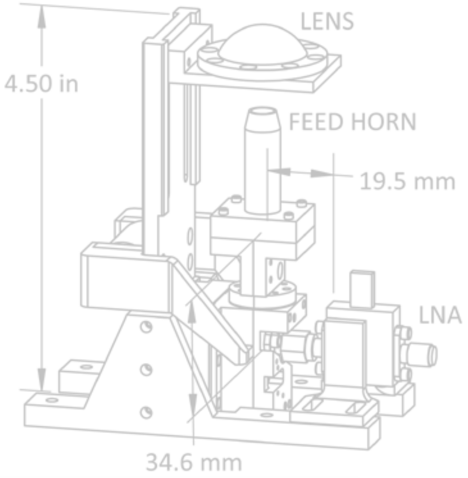

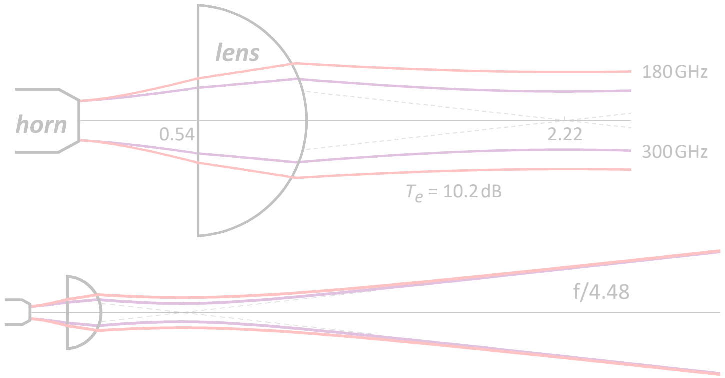

Observations

$$Y_{(m,m')} = \frac{-j}{2(m'V_{ph}+V_{if})} \sum_{k=-\infty}^{\infty} C_{(k)} C^*_{(k+m-m')} \begin{bmatrix} I(V_0+kV_{ph}) - \\ I(V_0+kV_{ph}-m'V_{ph}-V_{if}) + \\ I^*(V_0+(k+m-m')V_{ph}) - \\ I^*(V_0+(k+m-m')V_{ph}+m'V_{ph}+V_{if}) \end{bmatrix}.$$

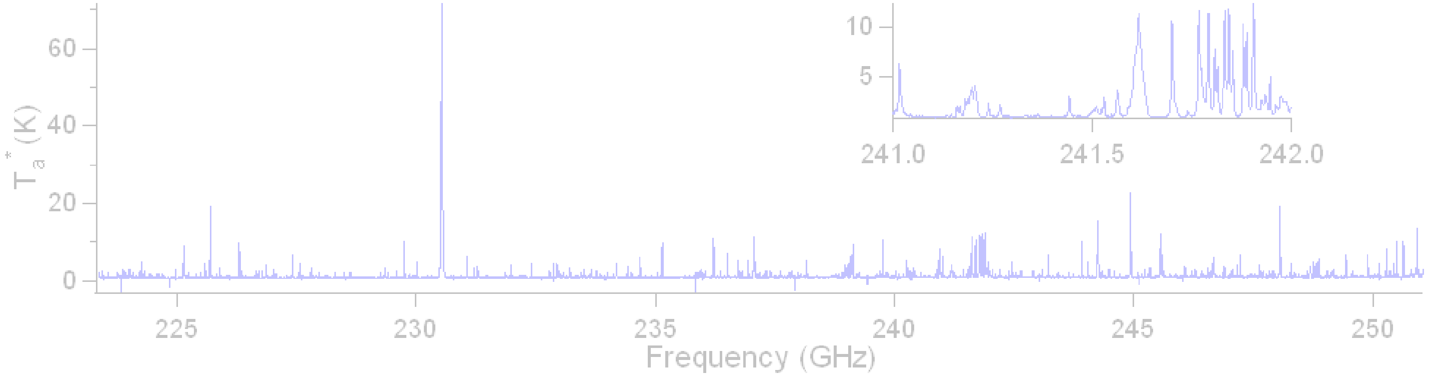

Spectral Line Surveys with the CSO

Susanna L. Widicus Weaver, Department of Chemistry, Emory University

Matthew Sumner, Frank Rice, Jonas Zmuidzinas, Department of Physics, Caltech

Geoffrey Blake, Department of Geological & Planetary Sciences, Department of Chemistry, Caltech

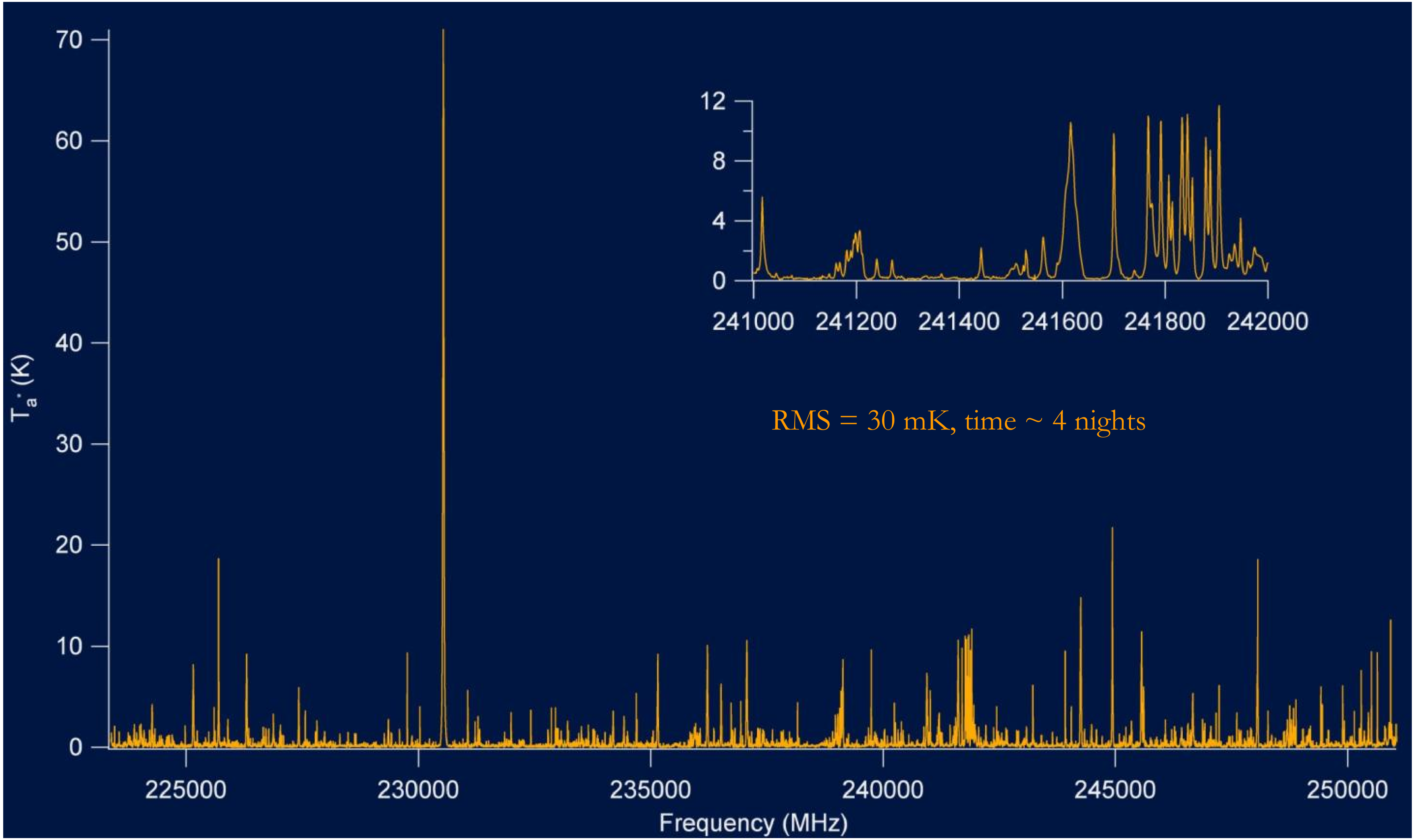
70
60
50
40
30
20
10
0
Ta* (K)
225000
230000
235000
240000
245000
250000
Frequency (MHz)
12
8
4
0
241000
241200
241400
241600
241800
242000
RMS = 30 mK, time ~ 4 nights

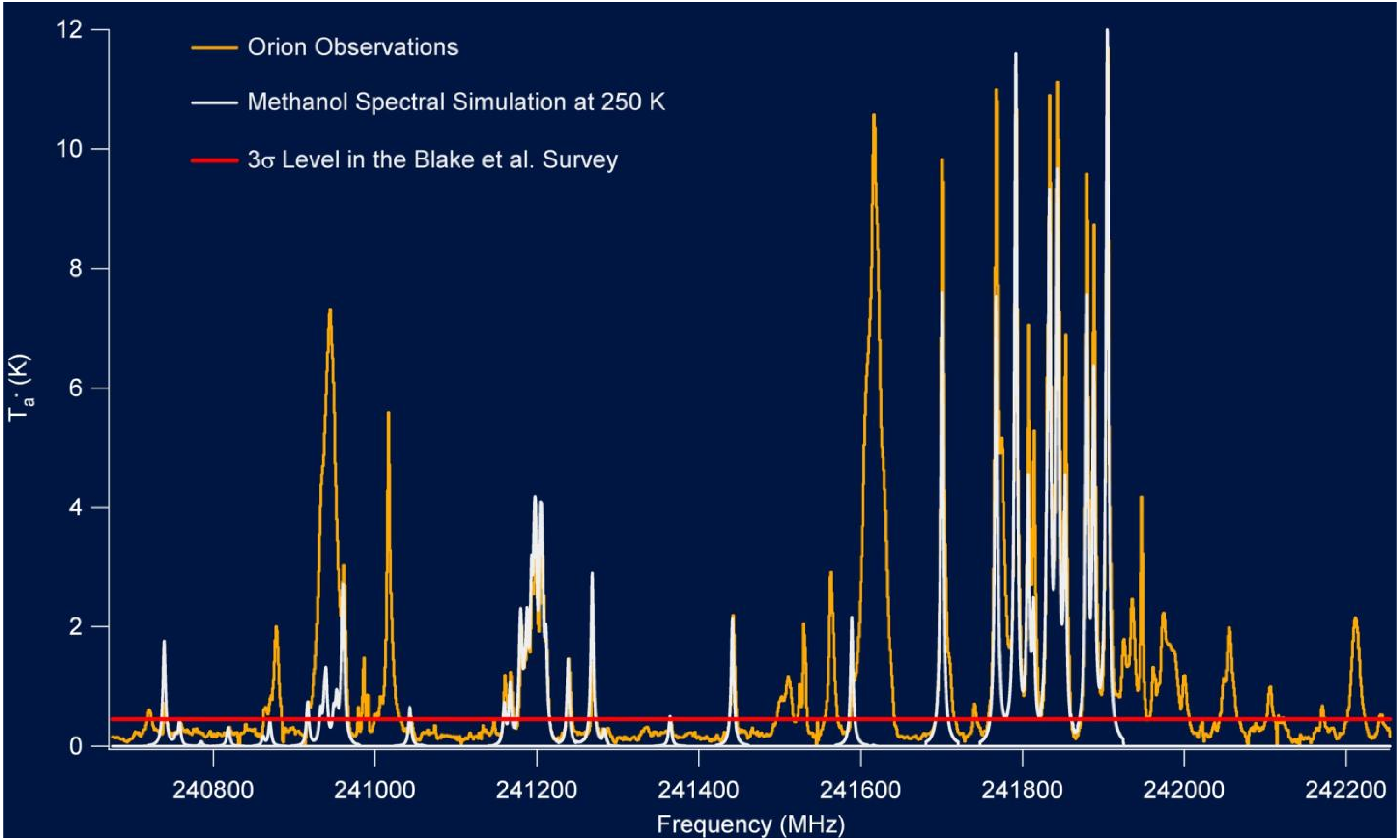

Orion Observations
Methanol Spectral Simulation at 250 K
3σ Level in the Blake et al. Survey
T_a^* (K)
0
2
4
6
8
10
12
240800
241000
241200
241400
241600
241800
242000
242200
Frequency (MHz)

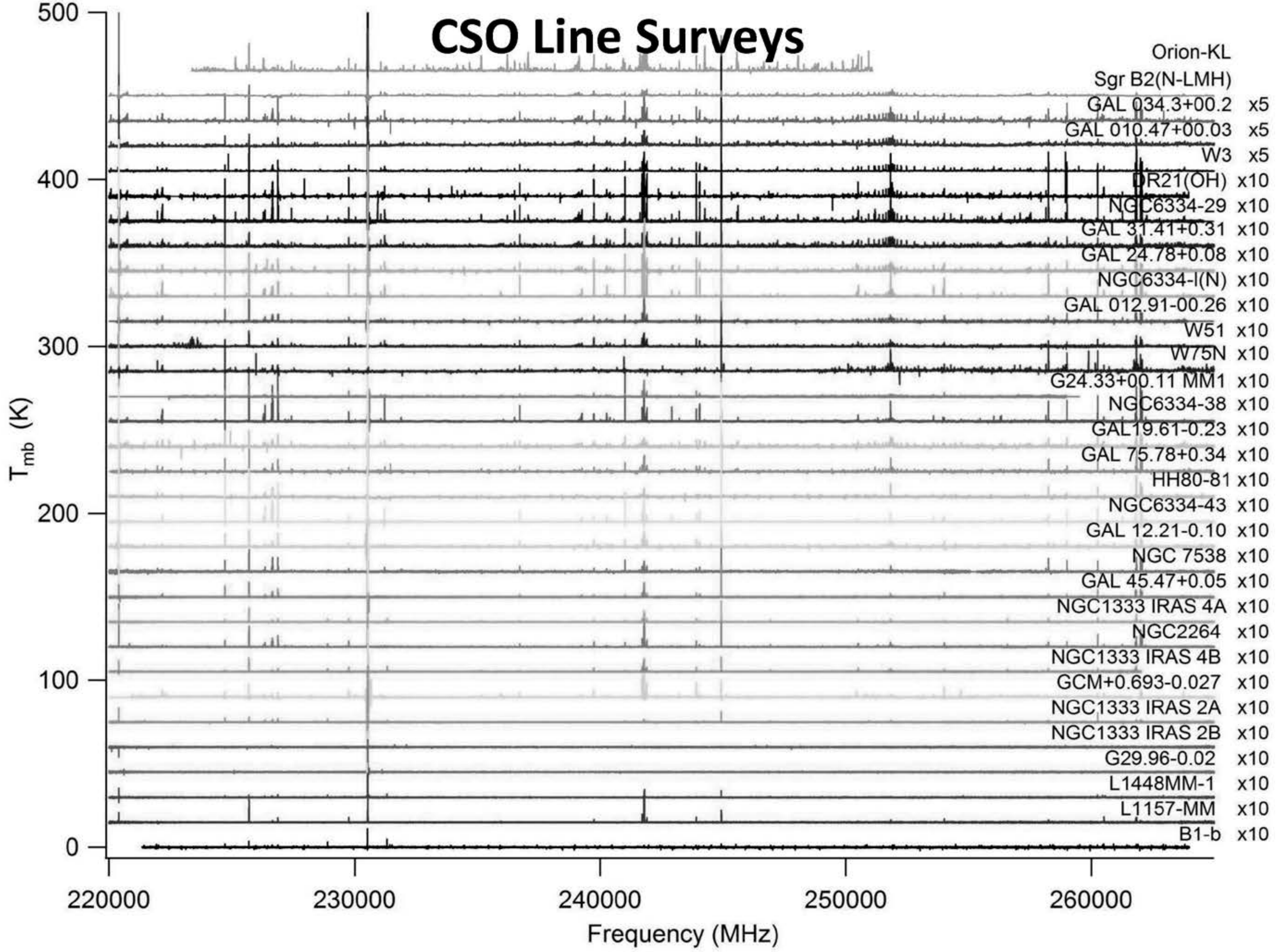
CSO Line Surveys
Orion-KL
Sgr B2(N-LMH)
GAL 034.3+00.2 x5
GAL 010.47+00.03 x5
W3 x5
DR21(OH) x10
NGC6334-29 x10
GAL 31.41+0.31 x10
GAL 24.78+0.08 x10
NGC6334-I(N) x10
GAL 012.91-00.26 x10
W51 x10
W75N x10
G24.33+00.11 MM1 x10
NGC6334-38 x10
GAL19.61-0.23 x10
GAL 75.78+0.34 x10
HH80-81 x10
NGC6334-43 x10
GAL 12.21-0.10 x10
NGC 7538 x10
GAL 45.47+0.05 x10
NGC1333 IRAS 4A x10
NGC2264 x10
NGC1333 IRAS 4B x10
GCM+0.693-0.027 x10
NGC1333 IRAS 2A x10
NGC1333 IRAS 2B x10
G29.96-0.02 x10
L1448MM-1 x10
L1157-MM x10
B1-b x10
T_{mb} (K)
0
100
200
300
400
500
220000
230000
240000
250000
260000
Frequency (MHz)